Hindawi
Shock and Vibration
Volume 2021, Article ID 8767592, 15 pages
https://doi.org/10.1155/2021/8767592

Review Article

Experimental Study of Strain Rockburst considering Temperature Effect: Status-of-the-Art and Prospect

Lei Xu [1] **and Fengqiang Gong** [1,2]

[1]*School of Resources and Safety Engineering, Central South University, Changsha 410083, China*
[2]*School of Civil Engineering, Southeast University, Nanjing 211189, China*

Correspondence should be addressed to Fengqiang Gong; fengqiangg@126.com

Received 15 August 2021; Accepted 16 October 2021; Published 10 November 2021

Academic Editor: Xing-Dong Zhao

In deep mining and excavation of tunnels with high geothermal, the surrounding rock is not only subjected to high ground stress but also subjected to high temperature. Temperature will change mechanical characteristics and energy storage capacity of rocks, as well as increase the destructiveness and randomness of rockburst. To reveal the mechanism of high-temperature strain burst in deep rock, the rockburst tests from uniaxial compression to three-dimensional compression were reviewed, and the research results of the minimum principal stress rapid unloading, true-triaxial loading with one free face, and dynamic disturbance triggered pre-heated granite rockburst simulation tests were focused on. According to the occurrence state of country rock for deep high-temperature and stress state in the whole process during excavation, six development directions for high-temperature strain rockburst simulation tests were proposed: (1) constructing the damage constitutive models of high-temperature rocks according to linear energy dissipation law; (2) developing the true triaxial rockburst simulation testing system accomplishing the function of "real-time high temperature + unloading + dynamic disturbance"; (3) considering the true triaxial rockburst simulation test after microwave irradiation; (4) developing the real-time high-temperature rockburst simulation testing device for large-size specimens and internal unloading; (5) focusing on the energy actuating mechanism for deep high-temperature rock failure via rockburst simulation tests; and (6) implementing the three-dimensional rockburst simulation test on the basis of deep in situ coring.

1. Introduction

Rockburst is an engineering geological disaster on account of deep rock excavating [1–6], which will cause great harm to the safety of personnel and equipment. With the depth increasing, not only the in situ stress rises significantly but also the ground temperature increases significantly [7–11]. In the construction of the Bulungkol-Gongur hydropower station, the tunnel's surrounding rock temperature is as high as 105°C and the maximum in situ stress is approximately 50 MPa [12]. Meanwhile, a host of tunnels in areas with high ground temperature also experienced severe and frequent rockburst disasters. For instance, the Gaoligong mountain tunnel, the longest railway tunnel in China, has the characteristics of high geothermal, high seismic intensity, and high ground stress; its maximum buried depth is 1155 m, the groundwater temperature is as high as 102°C, and rockburst disasters occur frequently [13]; the Sangzhuling tunnel, which belongs to China's Sichuan-Tibet Railway, has a temperature of 89°C in surrounding rock, the number of rockburst can reach more than 90,000 times and the length of the rockburst section accounts for 55% of the total length [14–16]. Figure 1 shows the on-site surrounding rock temperature and rockburst of the Sangzhuling tunnel. The occurrence principle of these rockburst disasters is bound up with high stress and high ground temperature. The high ground temperature will change the rocks' mechanical and energy storage peculiarities and aggravate the destructiveness and uncertainty of rockburst. Therefore, determining the mechanism of temperature on rockburst can provide an important reference for preventing and warning of rockburst disasters in deep mining as well as tunnels with high ground temperature.

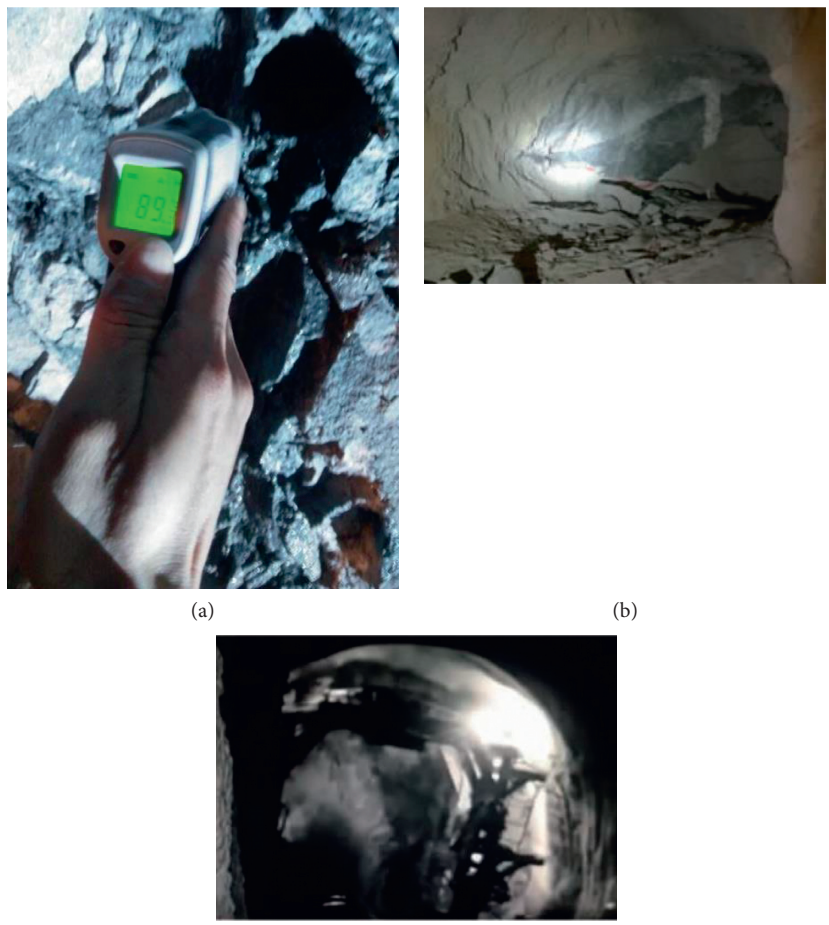

(a) (b)

(c)

Figure 1: Rock temperature and rockburst disasters in the Sangzhuling tunnel: (a) on-site rock temperature test photo [14]; (b) rockburst photo of tunnel arch foot [16]; (c) instant rockburst photo of tunnel vault [16].

Mechanical tests are the crucial means to explore the mechanism of rockburst and simulate the phenomenon of rockburst [17–25]. In the study of high-temperature rock mechanics, many scholars also investigate the temperature effect on strain rockburst through mechanical tests [10, 26–30]. The early uniaxial compression (UC) mechanical testing machine could not provide real-time high-temperature conditions; hence, the rock specimens were pre-heated first, and then the UC test was performed on the pre-heated specimens to explore the temperature effect on rockburst proneness. As the real-time high-temperature UC test system emerges, the study on rockburst proneness of high-temperature rock materials under UC comes into being. Although UC testing is the most conventional and effective way for exploring rocks' burst proneness under the condition of unknown in situ stress [31], the stress state of real-time high-temperature UC cannot truly reflect the actual stress environment and state of deep high-temperature rocks. Therefore, many experts have begun to explore the rockburst for pre-heated rocks under three-dimensional compression, e.g., the minimum principal stress rapid unloading test under triaxial compression [27, 28], the true triaxial loading with one free face test [29, 32], and the rockburst simulation test of granite with different thermal damage triggered by dynamic disturbance [30]. The above triaxial compression tests well reproduce the rockburst failure phenomenon of hard rock after preheating, whereas there is still a certain difference from the actual situation (real-time high-temperature) of the deep surrounding rock. For this reason, the occurrence environment of the deep surrounding rock, as well as stress characteristics of the whole process during excavation, must be taken into consideration before the high-temperature rockburst simulation test. On this basis, the development of a mechanical testing machine meeting the requirements of "real-time high-temperature + unloading + dynamic disturbance" can better reveal the mechanism of strain burst in deep high-temperature rocks.

Firstly, the rocks' peak compressive strength (σ_c), tensile strength (σ_t), elastic modulus (E), and energy storage capacity (ESC) at various temperatures were reviewed. Secondly, the rockburst simulation tests of pre-heated rocks under UC, triaxial compression rapid unloading, true-triaxial loading with one free face, and coupled dynamic-static loading were introduced and summarized. Finally, the simulation tests of high-temperature strain burst were prospected.

2. Temperature Effect of Mechanical Changes and Energy Characteristics for Rocks

The mechanical characteristics and ESC of rocks are closely related to the rockburst proneness [33–35]. To deeply understand and reveal the internal mechanism of temperature controlling, rock changes can offer a strong guarantee to reliability and security of high-temperature rock engineering. Recently, a large number of scholars have used acoustic emission (AE) [36, 37], optical microscopy [38, 39], scanning electron microscope [40, 41], CT scanning [42], and other means to observe the temperature effect on rocks' internal composition and structure. It is believed that under the thermal effect of rock, there are two aspects of consensus: on the one hand, the thermal dilation of mineral particles will result in microcracks' formation; on the other hand, the inconsistent deformation of mineral particles will further promote the expansion of existing microcracks. In addition, high temperature can give rise to destruction of internal structure and volatilization of mineral components for rocks; typically at 573°C, quartz will undergo a phase transition from α to β, and at 700°C, calcite will undergo thermal decomposition [40]. The expansion of thermal cracks, the destruction of internal structures, and the volatilization of mineral components are all important manifestations of rock damage. Without considering the effects of thermal shock, thermal cycling, and cooling rate, Wong et al. [43] summarize the thermal damage mechanism of rocks below 800°C under slow heating conditions, as shown in Figure 2.

The deterioration of rock properties is the macroscopic manifestation of internal thermal damage. Thermal damage will significantly reduce the P-wave velocity, σ_c, σ_t, and E of rocks [44, 45]. To observe the variable trend of σ_c, σ_t, and E with temperature changing, the statistical data were normalized; that is, the ordinate is the ratio of mechanical parameters under various temperatures to those under room temperature (RT), as shown in Figure 3. Through the statistical data of related scholars [46–48], it can be found that within a certain temperature range, the temperature often has a certain positive feedback effect on rocks. Specifically, as temperature increases, the σ_c, σ_t, and E of rocks first rise and subsequently decrease, which can be roughly divided into three intervals (Figure 3). Notably, the variation of the σ_c, σ_t, and E of rocks is not synchronous; for the σ_c, the threshold temperature is approximately 300°C, while for σ_t and E, the threshold temperature is approximately 400°C. The above results indicate that the temperature effect can significantly affect its mechanical properties.

Moreover, the energy evolution also changes significantly with the effect of high temperature. Xu et al. [46] obtained the three kinds of energy densities (total input strain energy density, elastic strain energy density, and dissipated strain energy density: u_t, u_e, and u_d, respectively) of pre-heated granite under various stress levels through the single-cycle loading-unloading UC test and curve integration method and analysed the energy distribution of pre-heated granites at various temperatures (20, 100, 300, 500, and 700°C). The results depicted that the pre-heated granites also have the same energy property as the RT rocks, that is, they possess linear energy storage and dissipation laws (Figure 4). The linear fitting equations between the u_e and u_t and u_d and u_t of pre-heated granite at different temperatures are shown in Table 1 (the coefficient of determination R^2 all above 0.9828). Hereafter, we defined the compression energy storage coefficient (A) to represent rocks' ESC, as well as the compression energy dissipation coefficient ($1–A$) to represent their energy dissipation capacity (EDC) [21, 33]. Figure 5 demonstrates the variations of the A and $1–A$ for pre-heated granite specimens in response to temperature.

3. Research Progress of Strain Rockburst Test considering Temperature Effect

3.1. Rockburst Proneness of Pre-Heated Granite under UC. To investigate the temperature effect on rock materials' burst proneness, Xu et al. [41] adopted common granites in underground high-temperature rock engineering as test objects. Starting from the characteristics for energy storage, dissipation, and residue during rock failure, the rockburst proneness of pre-heated granite specimens was analysed accurately and quantitatively by ejection mass ratio outside the indenter (M_E) and residual elastic energy index (A_{EF}). Firstly, the granite was pre-heated at 20, 100, 300, 500, and 700°C, respectively; the single-cycle loading-unloading test was used to separate u_e and u_d of the pre-heated granite specimens under different stress levels. Meanwhile, semi-quantitative criterion, M_E, to evaluate the severity for pre-heated granite failure was used (Figure 6). Secondly, by analysing the relationship between u_e and u_t of specimens, it is clear that the pre-heated granites possess the linear energy storage law (Figure 4(a)). On this basis, u_e at peak strength (u_e^p) of pre-heated granites was accurately calculated. Importantly, A_{EF} was used to quantitatively characterize the rockburst proneness of pre-heated granite specimens under various temperatures, as shown in Figure 7.

Finally, the consistency between the evaluation results and the actual failure severity was compared of specimens, and it was found that the statistical results M_E and discrimination results A_{EF} of pre-heated granite at different temperatures had a good correspondence relationship (Figure 8). The results illustrated that A_{EF} can precisely and quantitatively characterize the rockburst proneness of pre-heated granites at different temperatures. The discriminant results were as follows in order of temperature: 300°C (317.9 kJ/m^3), 100°C (264.1 kJ/m^3), 20°C (260.6 kJ/m^3), 500°C (245.5 kJ/m^3), and 700°C (158.9 kJ/m^3); the rockburst proneness of pre-heated granites at 300°C was the highest. In addition, the ESC, σ_c, and the relationships among the related parameters and rockburst proneness of pre-heated granite at different temperatures were analysed, and the essential reason of which the rockburst proneness first enhanced and then weakened as the temperature increases was revealed.

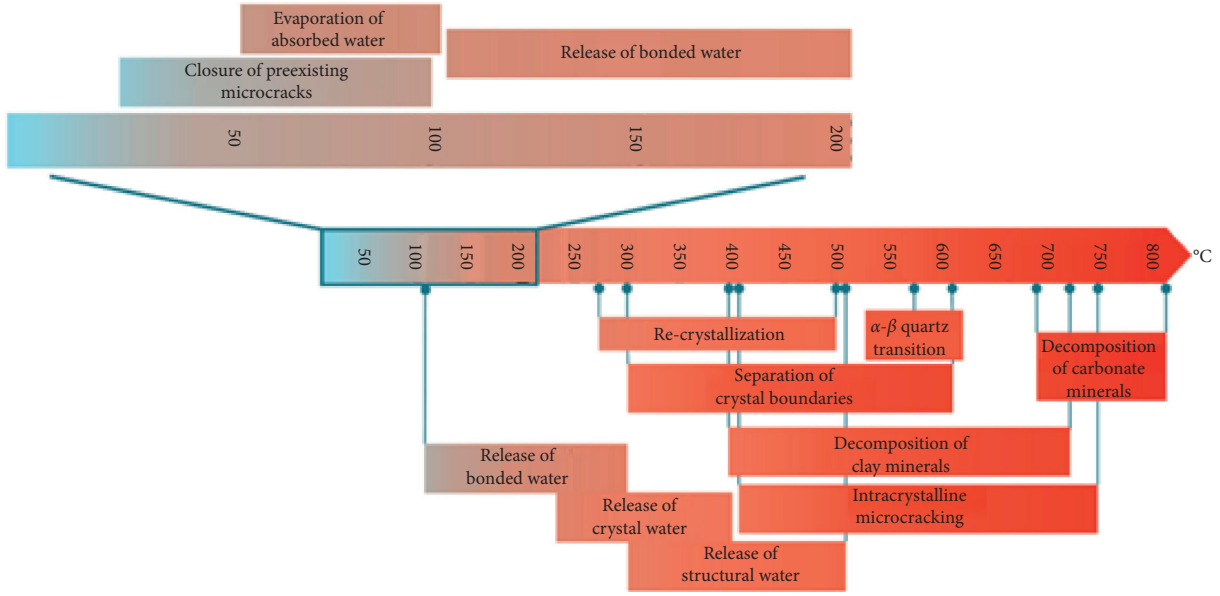

Figure 2: Variations of internal composition and structure of rocks at different temperatures [43].

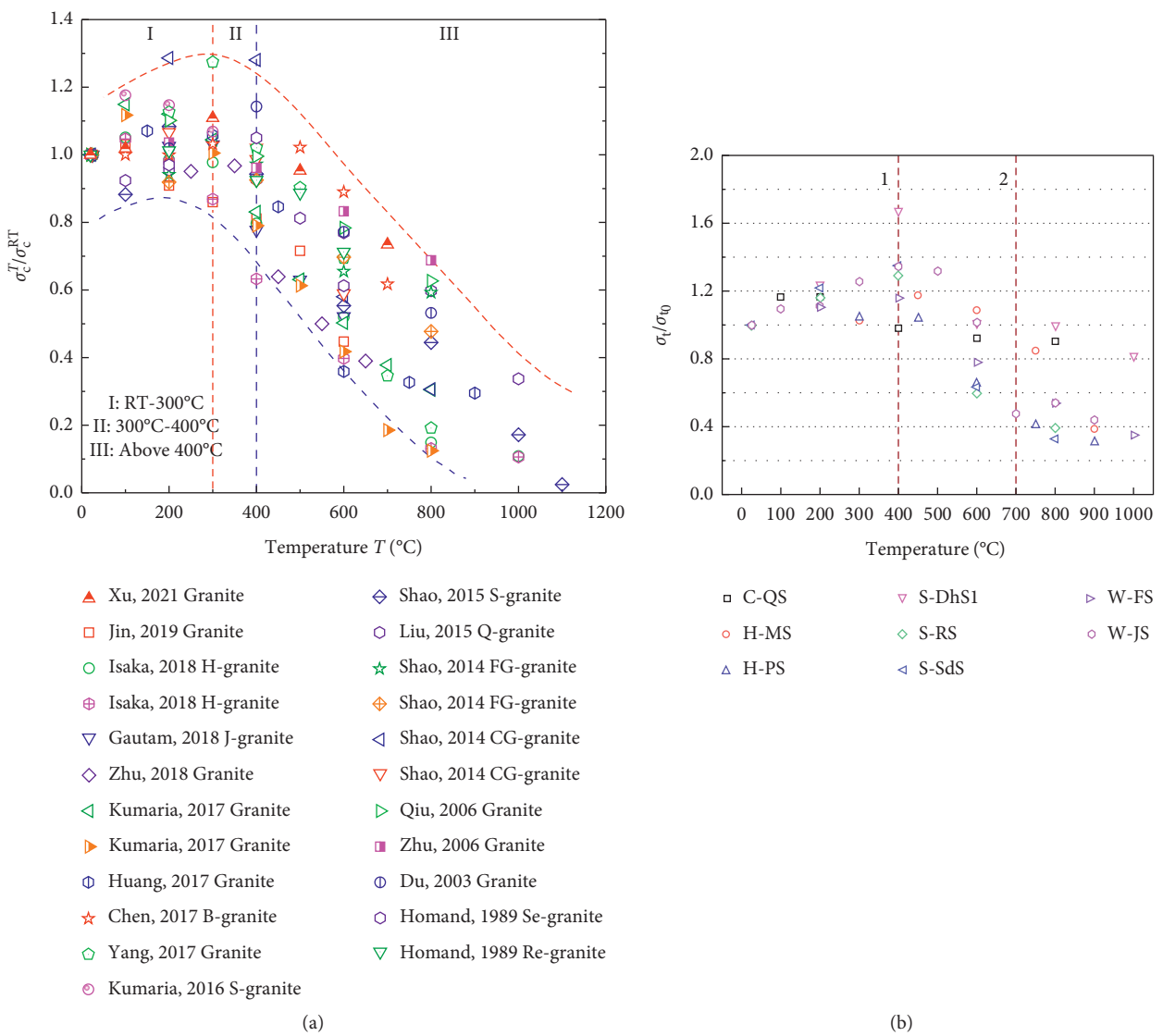

Figure 3: Continued.

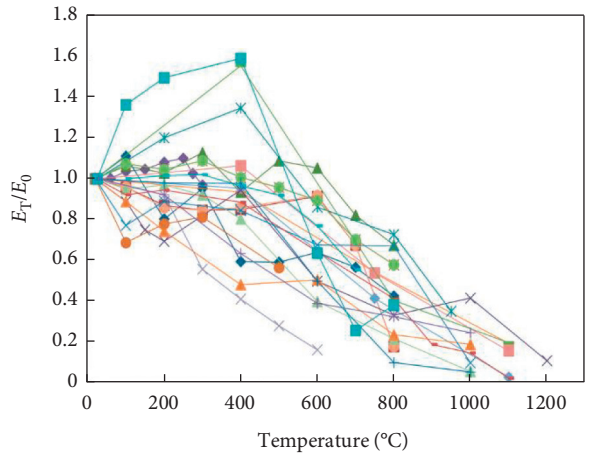

(c)

Figure 3: Mechanical parameters at different temperatures: (a) peak compressive strength σ_c [46]; (b) tensile strength σ_t [47]; (c) elastic modulus *(E)* [48].

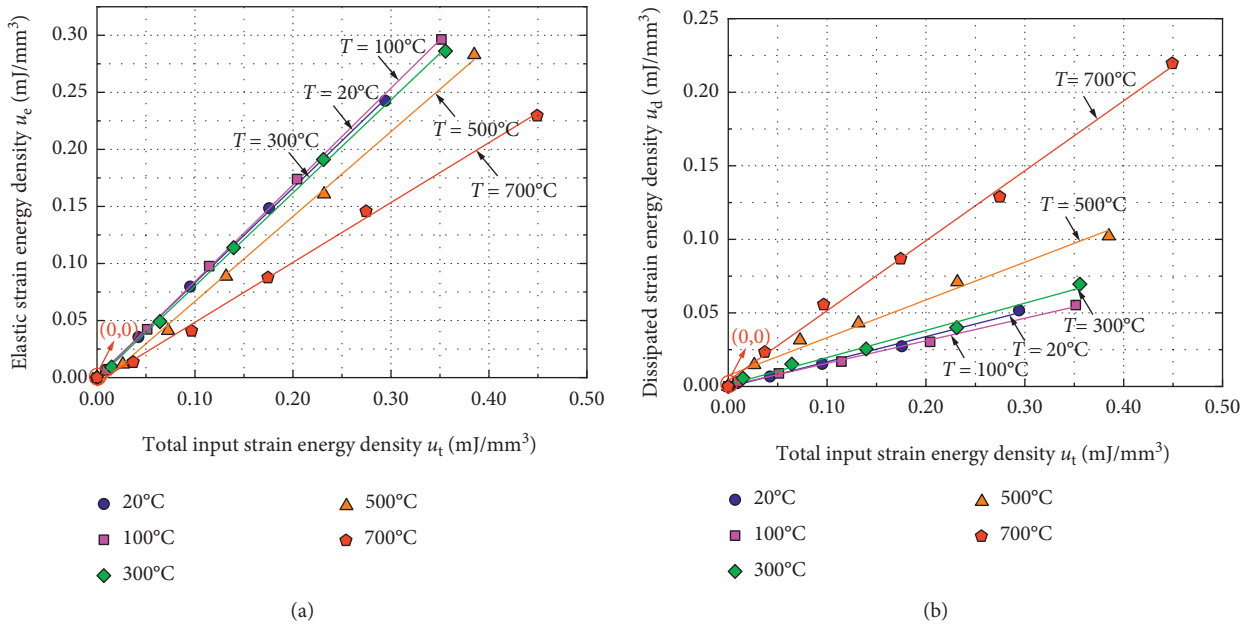

(a) (b)

Figure 4: Relationships between the three energy densities of pre-heated granite specimens (the linear fitting results of u_e and u_t (a) and u_d and u_t (b) are shown) [46].

Table 1: Linear fitting equations between u_e and u_t and u_d and u_t of pre-heated granite specimens [46].

Temperature (°C)	Linear fitting function between u_e and u_t	Linear fitting function between u_d and u_t
20	$u_e = 0.8285u_t + 0.0004$, $R^2 = 0.9998$	$u_d = 0.1715u_t - 0.0004$, $R^2 = 0.9947$
100	$u_e = 0.8468u_t - 0.0004$, $R^2 = 0.9999$	$u_d = 0.1532u_t + 0.0004$, $R^2 = 0.9971$
300	$u_e = 0.8152u_t - 0.0012$, $R^2 = 0.9995$	$u_d = 0.1848u_t + 0.0012$, $R^2 = 0.9902$
500	$u_e = 0.7435u_t - 0.0075$, $R^2 = 0.9979$	$u_d = 0.2565u_t + 0.0075$, $R^2 = 0.9828$
700	$u_e = 0.5246u_t - 0.0040$, $R^2 = 0.9977$	$u_d = 0.4754u_t + 0.0040$, $R^2 = 0.9972$

3.2. Rockburst Proneness of Real-Time High-Temperature Granite under UC. To explore the temperature effect of rockburst proneness in deep-buried tunnels, Chen et al. [10] adopted the MTS 815 mechanical testing system to carry out UC tests on high-temperature granite specimens (diameter 50 mm × height 100 mm). The granite specimens were taken from the railway tunnel from Dali to Ruili in southwestern China. Five temperature gradients were set at 20, 40, 60, 90,

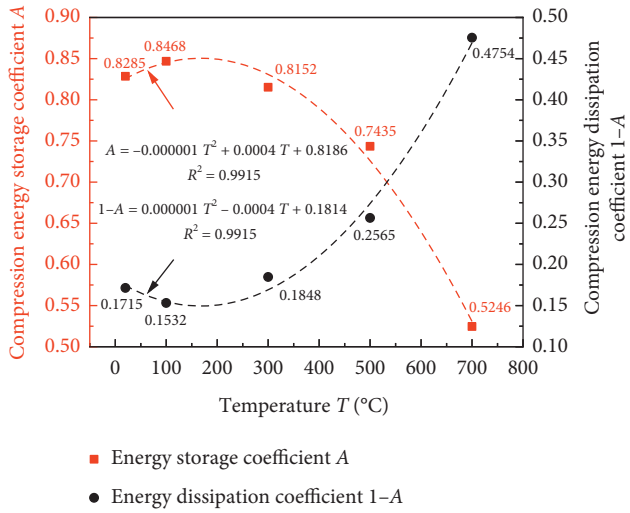

FIGURE 5: The variations of A and $1-A$ for pre-heated granite specimens [46].

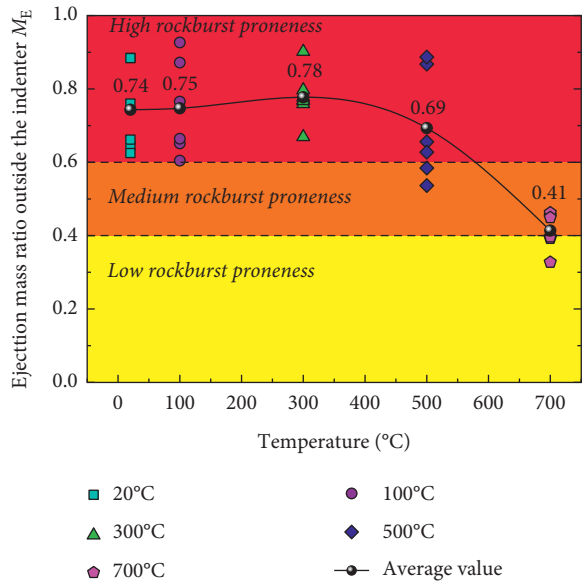

FIGURE 6: M_E of pre-heated granite specimens under various temperatures [46].

and 130°C. To guarantee even heating of granites, they were first heated to target value then kept constant for two hours before the test. First, the UC test was performed on specimens to obtain the σ_c at this temperature; then, they assessed the granites' burst tendency at different temperatures by strain energy storage index W_{et} [49]. Specifically, the granite specimen was loaded to approximately 80% of the σ_c and then unloaded to obtain the u_e and u_d during specimens' prepeak stage. It was found that below 130°C, W_{et} of granite specimen was higher than 5.0 (Figure 9); these results demonstrated that all granite specimens tested possess strong burst proneness.

At the same time, to explore the energy release during rock failure, Chen et al. [10] also used AE equipment to monitor the transient energy released during failure.

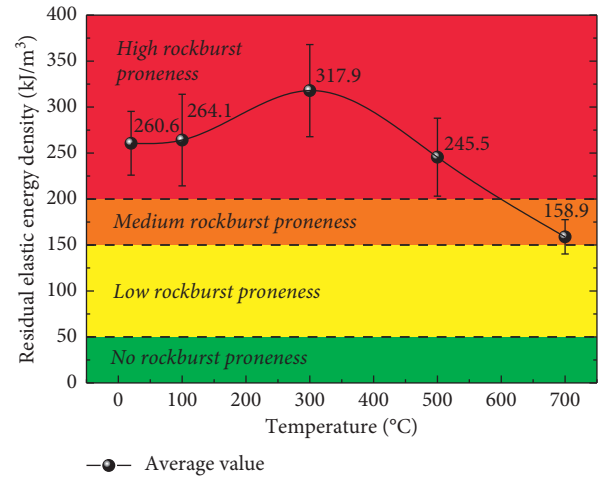

FIGURE 7: A_{EF} of pre-heated granite specimens under various temperatures [46].

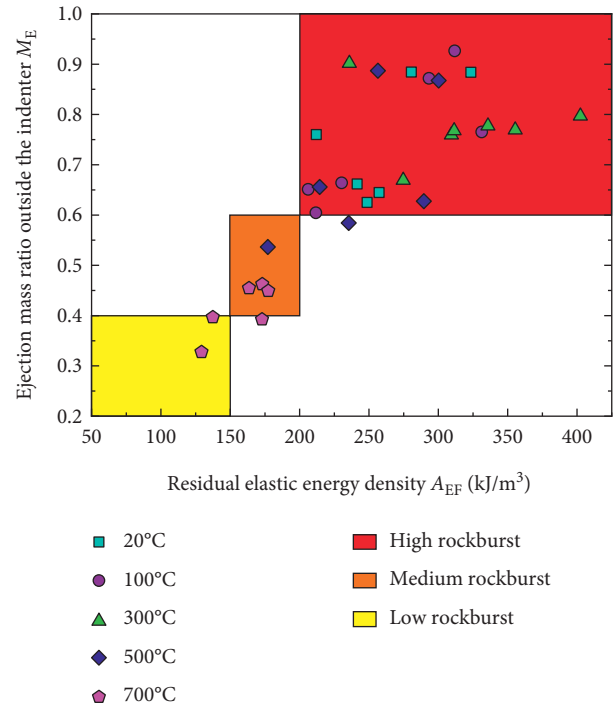

FIGURE 8: Relationship between M_E and A_{EF} [46].

Through comprehensive analysis of W_{et} and AE energy release (Figure 9), it was found that, in the range of 20–60°C, the intensity of brittle failure of rock gradually enhanced as temperature increased; above 60°C, brittle failure was gradually transformed to brittle-plastic one, while the specimens at all temperatures showed a strong burst proneness. Subsequently, Chen et al. [50] evaluated the brittleness of granite at RT to 130°C in order to further explore the mechanism of hard rockburst in a high-stress and high-temperature environment. By analysing the brittleness index P_f of rocks at different temperatures

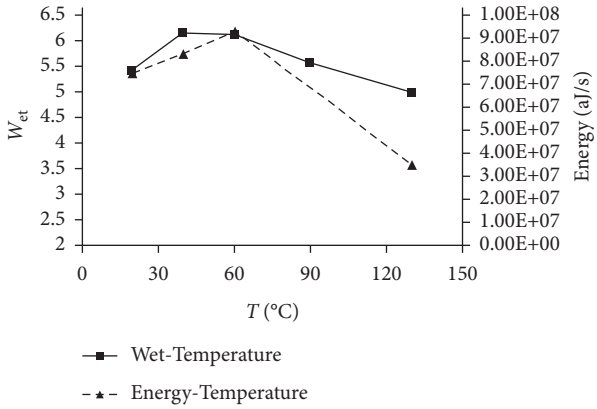

Figure 9: Strain energy storage index W_{et} and energy release of rocks at different temperatures [10].

(Figure 10), it was found that the brittle failure of rocks below 60°C was significantly higher than that at RT. Obviously, thermal stress will enhance the strength and ESC of hard rocks.

3.3. Rockburst Test of Pre-Heated Granite under "True Triaxial Compression + Rapid Unloading". Since the deep undisturbed rock is not only influenced by temperature but by three-dimensional high ground stress, excavation of the rock mass will produce free faces and form internal spaces, which will lead to surrounding rock's stress redistribution (Figure 11). Accompanied by high ground stress and high temperature, the elastic strain energy inside the surrounding rock gradually accumulates after excavation, and eventually, rockburst disaster occurs. Therefore, to simulate the rockburst disaster caused by the excavation response of deep high-temperature rock, He et al. [51] exploited a rockburst test system (Figure 12). This can realize three-way asynchronous loading and unloading, as well as the fast synchronous loading and unloading on any two faces. Based on this, Akdag et al. [27] conducted strain burst tests on pre-heated granite specimens (125 mm × 50 mm × 25 mm) at 25, 50, 75, 100, 125, and 150°C. Figure 13 depicts the tested stress path and loading-unloading methods. To accurately reflect the stress adjustment and stress concentration during excavating, 17 MPa/s was used to unload σ_3 while maintaining σ_2; then, 0.25 MPa/s was applied to load σ_1 until the strain burst was triggered. The results indicated that, in the range of 25 to 150°C, 100°C was considered as the threshold temperature of strain burst. From 25 to 100°C, the stress and ejection kinetic energy decreased gradually; while above 100°C, they increased. Specifically, high temperature promotes the thermal expansion of internal grains, making the specimen to become denser. Notably, it means that the deeper the excavation is, the higher the temperature of the rock mass will be, which may trigger more serious rockburst disasters.

Subsequently, Ren et al. [28] introduced the binocular stereovision technology (Figure 14) to determine the velocity distribution situations for rock fragment ejection more accurately and quantitatively during rockburst of the pre-heated rock. Based on a stress path which is similar to that shown in Figure 13, they executed rockburst simulation tests on pre-heated specimens (150 mm × 60 mm × 30 mm) at 25, 50, 100, and 150°C, separately. The ejection path of the strain burst of the typical specimen under various temperatures is depicted in Figure 15. According to this technology, the ejection velocity, particle size distribution, and ejection kinetic energy in pre-heated granite burst were basically determined. The results demonstrated that rock pieces' velocity and particle size distribution during burst have a log-normal distribution. As the temperature rises, the intensity of rockburst enhances, which can be seen in views of the rockburst pit's volume, debris' fractal feature, and kinetic energy.

3.4. Rockburst Test of Pre-Heated Granite under True Triaxial Loading with One Free Face. Rockburst is bound up with stress as well as the high temperature environment of country rock after excavation. After being excavated, the rock at the boundary will undergo stress redistribution (Figure 11); that is, the radial stress of the free face does not anymore, whereas the stress along the tunnelling direction still exists. Traditional rockburst simulation tests often focus on the maximum stress's influence, whereas do not consider the stress state of excavation boundary. Meanwhile, the single loading face rapid unloading test also cannot reproduce this stress state perfectly. Therefore, in order to simulate the strain burst caused by tangential stress concentration after high-temperature granites excavating, Su et al. [29, 32] developed a rigid rockburst test system (Figure 16(a)), which adopted the method of "true-triaxial loading with one free face" to accurately reflect the force characteristics for excavation boundary (Figure 11). The rockburst simulation tests of pre-heated granite specimens (200 mm × 100 mm × 100 mm) at different temperatures were carried out by using this test system. First, Su et al. [29] heated the granite specimens to 100, 200, 300, 400, 500, 600, and 700°C to obtain the pre-heated specimens. Second, based on the stress path in Figure 16(b), the rockburst test was carried out on this rigid system. Meanwhile, the high-speed camera system is used to record pre-heated granites at different temperatures' rockburst phenomenon. Finally, the variations of failure mode, peak stress, peak strain, failure time, and ejection kinetic energy during rockburst with the increase of temperature were analysed. The results exhibited that temperature has a significant influence on strain bursts for pre-heated specimens. When the temperature is below 300°C, the intensity of rockburst increases gradually as temperature increases, and above 300°C, the intensity of rockburst decreases rapidly.

3.5. Rockburst Test of Thermal Damaged Granite under "True-Triaxial + Dynamic Disturbance". As a natural geological body, rock has many discontinuous defects inside, causing it to have certain initial damage.Blasting excavation will aggravateor cause the further damage of country rock. Regarding the force situations of deep rock, while enduring the static stress, it is also accompanied by the disturbing effect caused by blasting excavation (Figure 17(a)). Importantly, the damage inside a rock will be manifested in the

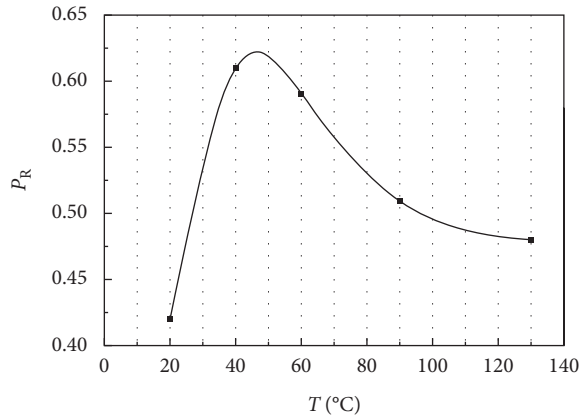

Figure 10: Brittleness index P_f of rocks at different temperatures [50].

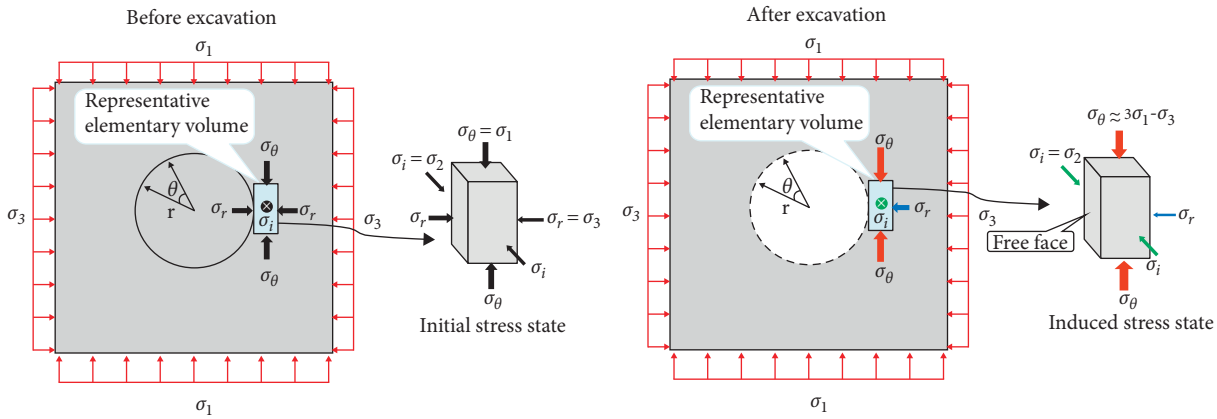

Figure 11: Schematic diagram of stress distribution on the tunnel wall before and after deep rock excavation [27].

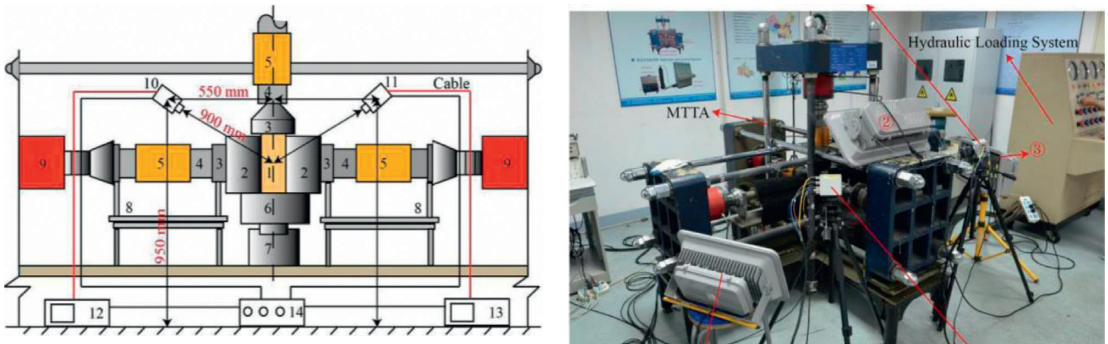

Figure 12: Schematic diagram of strain burst test system: (a) schematic diagram; (b) physical picture [28].

time, intensity, and scope of rockburst. To explore the effect of the initial damage for rock on remotely triggered burst, Jiang et al. [30] prepared granite specimens with initial thermal damage D of 0, 0.2, 0.3, 0.4, 0.6, and 0.7, by pre-heating treatment at 25, 200, 300, 400, 500, and 600°C, respectively. Then, based on the test system in Figure 16(a), the coupled static-dynamic test method (Figure 17) was adopted to trigger the rockburst of specimens with different thermal damage. The test results show that when the static stress exceeds a certain threshold, a dynamic disturbance will trigger rockburst for granites with initial thermal damage; as D rises, it is easier to trigger rockburst by dynamic

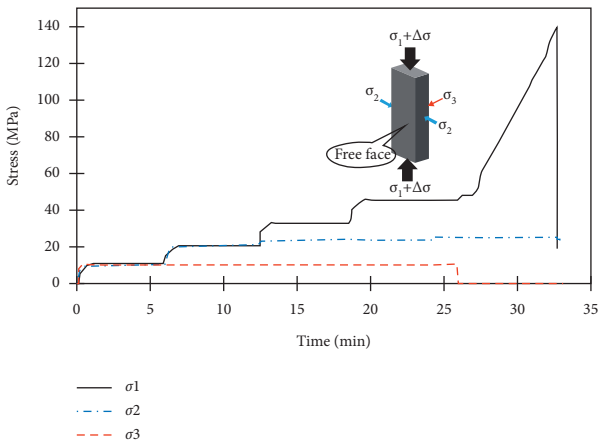

Figure 13: Stress path diagram of strain burst test under σ_3 rapid unloading [27].

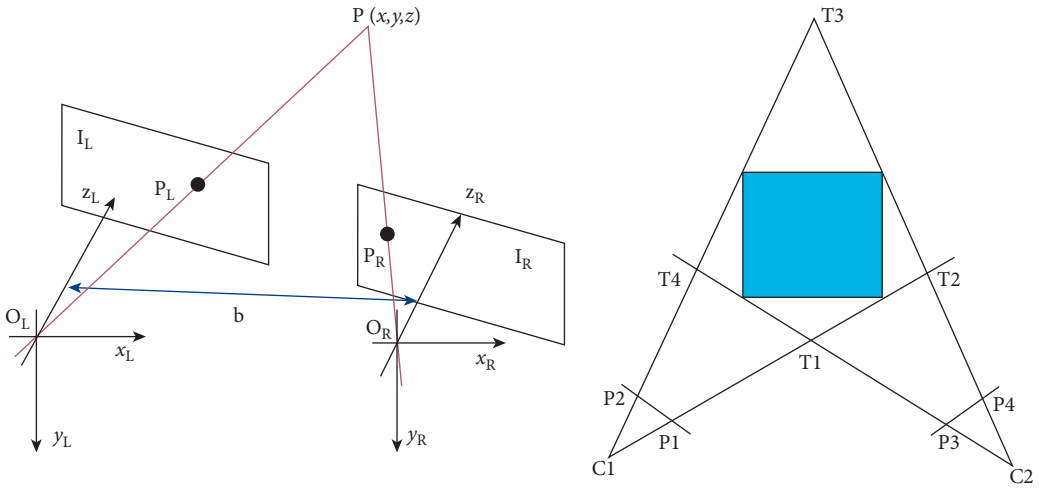

(a) (b)

Figure 14: Schematic diagram of binocular stereovision technology [28].

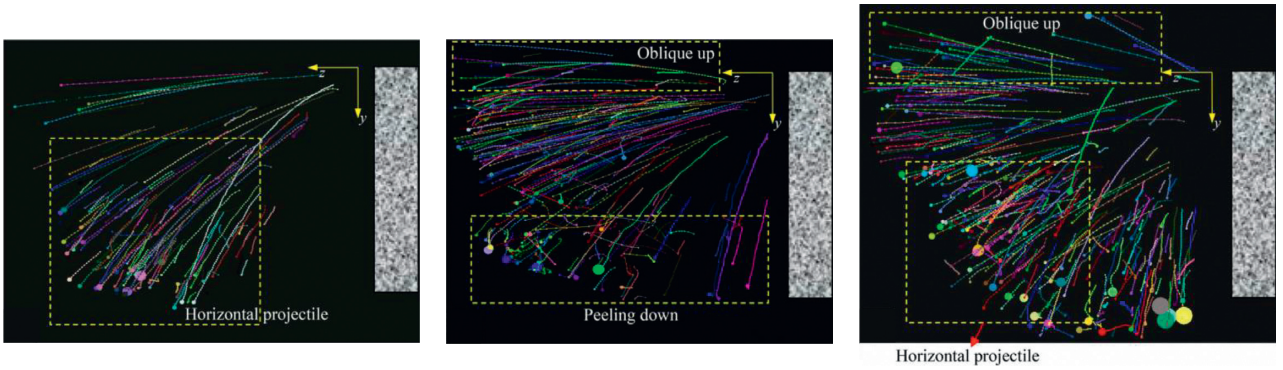

(a) (b) (c)

Figure 15: Continued.

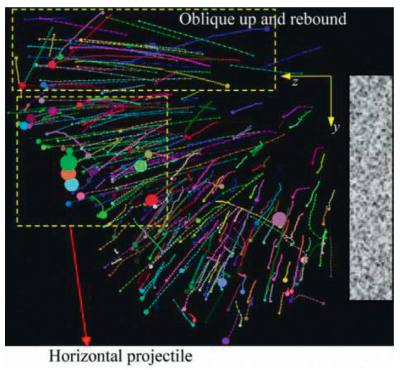

(d)

Figure 15: Ejection paths of typical pre-heated specimens during strain burst: (a) 25°C; (b) 50°C; (c) 100°C; (d) 150°C [28].

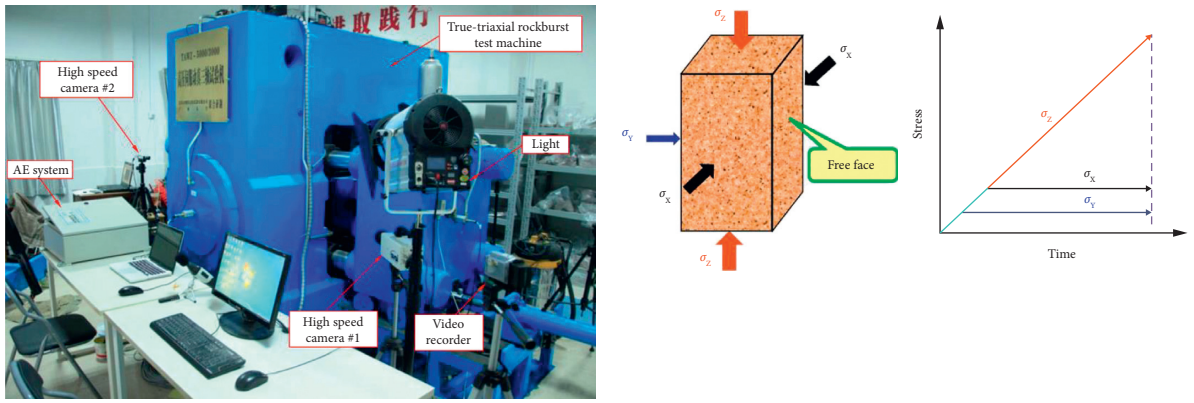

(a) (b)

Figure 16: Rockburst test system and loading mode: (a) physical picture; (b) stress path [29].

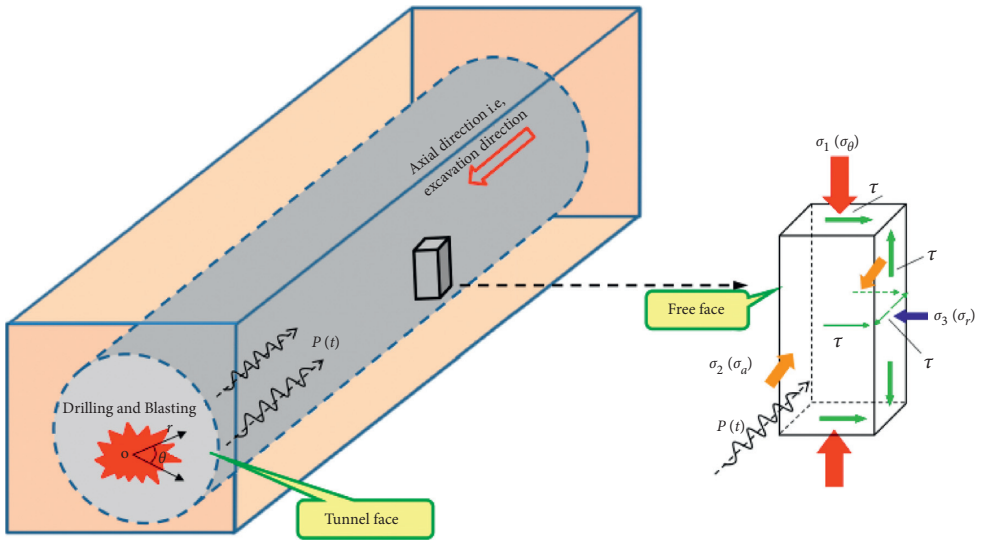

(a)

Figure 17: Continued.

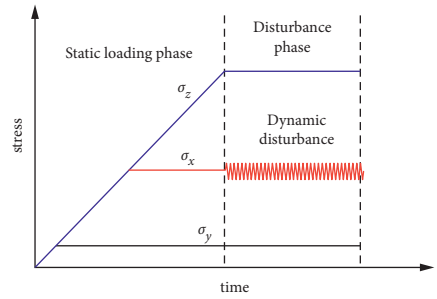

(b)

FIGURE 17: Mechanical analysis of rockburst simulation test for deep-buried tunnel: (a) the stress situation of tunnel free face; (b) the loading stress path [30].

disturbance. Importantly, the intensity of rockburst increases firstly and subsequently decreases as D increases, and the rockburst of granite is the most violent at $D = 0.3$. This is basically consistent with the test results obtained by Su et al. [29] and Xu et al. [46]; that is, when the temperature is 300°C, the rockburst intensity of rock is the largest, and it is speculated that 300°C may be the threshold temperature of rockburst.

4. Development Trend of Rockburst Test considering the Temperature Effect

Up to now, with the development of deep rock mechanics, great progress has been made in the simulation test of rockburst considering temperature effect, both in the development of test equipment and in the breakthrough work of high-temperature rock mechanics as well as the scholars' scientific understanding of strain burst in a high-temperature rock mass. According to the current rock mechanical test system's performance as well as the rockburst simulation test's progress, there are several prospects for the rockburst test considering the temperature effect:

(1) Constructing the damage constitutive models of high-temperature rocks according to linear energy dissipation law: according to the above research results, the high-temperature damage in deep rock engineering not only weakens the burst proneness of rock but to some extent will enhance the burst proneness of surrounding rock [26–30, 46]. Therefore, constructing the high-temperature damage constitutive model is a vital means to reflect the mechanical and deformation characteristics of high-temperature rock during failure. Many scholars have established these kinds of models from the microscopic perspective of statistical theory and achieved good results [52–54]. However, rockburst proneness or rockburst simulation test often analyzes the deformation and failure of rocks in the view of macroscopic (e.g., rock energy and failure characteristic); dissipated energy is the essence of gradual development for internal damage in rocks. Currently, the linear energy dissipation law of pre-heated granites has been confirmed (Figure 4(b)); based on this, the rocks' damage evolution and the constitutive equation can be obtained accurately [55, 56]. Therefore, if we could establish a simple, accurate, and applicable constitutive model in view of rock energy dissipation, the mechanism of temperature effect on strain burst can be better revealed.

(2) Developing the true triaxial rockburst simulation testing system and accomplishing the function of "real-time high-temperature + unloading + dynamic disturbance": for the existing true triaxial rockburst simulation test studies, most of them are unloading or dynamic disturbance rockburst tests on the pre-heated rock. The test research of rockburst under real-time high-temperature conditions is not yet mature. At present, the investigation of rockburst proneness under real-time high temperature has been successfully realized in the UC test. However, the deep rock is in a real-time high-temperature state while being under three-dimensional high stress. Under excavation and disturbance, the excavation (loading) rate [57] will also cause different mechanical responses to the surrounding rock. Therefore, there is an urgent need for a "real-time high-temperature + unlading + dynamic disturbance" three-dimensional testing equipment to truly achieve rockburst simulation under the conditions of deep high-temperature surrounding rock or geothermal tunnel excavation.

(3) Considering the true triaxial rockburst simulation test after microwave irradiation: microwave-assisted rock breaking has achieved good results in tunnelling and deep rock engineering. Microwave irradiation will alter rocks inside structure and mineral components, giving rise to obvious variations among properties, energy evolution, as well as failure modes. For the failure of the surrounding rock, the influence of microwave irradiation cannot be ignored. Therefore, if the conventional true-triaxial rockburst simulation test system can be further improved, the role of microwave irradiation will be considered, and then a favorable theoretical reference will be provided for the safety of engineering using microwave-assisted rock breaking.

(4) Developing the real-time high-temperature true triaxial rockburst simulation testing device for large-size specimens and internal unloading: at present, the rockburst test considering the temperature effect mainly focuses on complete small-sized rock specimens. It is well known that underground rock engineering is a spatial structure formed by excavation inside a rock mass. Conventional rockburst simulation tests adopt the method of "opening first, then loading," which only simulates the force situation of country rock in the deep roadway to a certain extent, which is quite different from the actual method of "loading first, then opening," and cannot reflect the force situation for surrounding rock during deep excavating. Si and Gong [58] have realized the rockburst simulation test of rocks' internal unloading under two-dimensional conditions on the TRW-3000 true triaxial (disturbance) test system, while the "real-time high-temperature + internal unloading + triaxiality stress" is a real state for deep high-temperature rock engineering excavation.

(5) Focusing on the energy actuating mechanism for deep high-temperature rock fracture via rockburst simulation tests: currently, most of the laboratory tests have well reproduced the rockburst process of pre-heated granite at different temperatures, whereas they cannot quantitatively describe the temperature effect of rockburst proneness. In essence, energy drive contributes to the rockburst, a kind of inside energy release's macroscopic manifestation [33, 51]. At RT, Gong et al. [21, 35] found that rock and coal specimens have linear energy storage law in the UC test, and on this basis, they defined the bursting proneness criterion of residual elastic energy index. With further exploration, it is found that the rocks possess the linear energy storage law in three-dimensional compression [59], preset angle shear test [60], and fracture test [61], as well as the pre-heated granite specimens in the UC test [46]. Therefore, when investigating the failure of deep high-temperature rock, adopting the linear energy storage law can accurately calculate extremity energy storage as well as residual elastic strain energy during the whole process, to realize the quantitative evaluation of rockburst proneness.

(6) Implementing the three-dimensional rockburst simulation test on the basis of deep in situ coring: in deep rock engineering, the country rock frequently suffers from high temperature, high seepage, high ground stress, and excavation disturbance's coupling effect. The most ideal condition for the laboratory test of deep rock mechanics is to obtain the test specimens according to the deep in situ coring technique proposed by Xie et al. [62, 63]. In situ coring basically maintains the deep environment and stress state, and characteristics of deep rocks under the condition of various temperatures, humidity, and pore pressures will be supplied. Based on this, the development of the rockburst simulation test has important reference value for not only assessment but also prevention of rockburst during deep rock engineering.

5. Conclusion

The obvious temperature effect can be found among the σ_c, σ_t, E, ESC, and EDC of rocks. Rockburst simulation tests for real-time high-temperature rocks under UC and pre-heated rocks under true-triaxial compression have achieved great success. Nevertheless, due to the limitation of the performance of the current mechanical testing machine and the test conditions, these reports of rockburst proneness under triaxial compression considering the effect of temperature are still focused on the small-sized rock specimens after preheating; it cannot simulate the real-time high-temperature environment of deep rocks and the stress state of internal excavation unloading. Specifically, conducting mechanical tests in real-time high-temperature is a prerequisite for the success of high-temperature rock mechanics. With deep rock mechanics developing and scientific understanding of high-temperature rock mechanics deepening, scholars have gradually realized that real-time high-temperature, large-sized specimens are the development direction of high-temperature rockburst simulation experiments. This study introduces the temperature effect towards rock materials' mechanic and energy parameters and summarizes the situation of rockburst simulation tests under UC and triaxial compression; in particular, the research progress of rockburst simulation tests of pre-heated rocks under triaxial compression, rapid unloading, and true-triaxial loading with one free face and different initial thermal damage are summarized. Finally, combining the actual occurrence environment and stress state of strain burst in deep surrounding rocks and high geothermal tunnels, the development trend and research direction of rockburst test considering the temperature effect are proposed.

Data Availability

All data used to support the findings of this study are included within the article.

Conflicts of Interest

The authors declare no conflicts of interest.

Acknowledgments

This work was supported by the National Natural Science Foundation of China (Grant no. 41877272), the Fundamental Research Funds for the Central Universities of Central South University (Grant no. 2021zzts0861), the Postgraduate Scientific Research Innovation Project of Hunan Province (Grant no. CX20210299), and the Fundamental Research Funds for the Central Universities of Southeast University (Grant no. 2242021R10080).

References

[1] W. D. Ortlepp and T. R. Stacey, "Rockburst mechanisms in tunnels and shafts," *Tunnelling and Underground Space Technology*, vol. 9, no. 1, pp. 59–65, 1994.

[2] E. Hoek, P. K. Kaiser, and W. F. Bawden, *Support of Underground Excavations in Hard Rock*, Taylor & Francis, Balkema, London, UK, 1995.

[3] P. G. Ranjith, J. Zhao, M. Ju, R. V. S. De Silva, T. D. Rathnaweera, and A. K. M. S. Bandara, "Opportunities and challenges in deep mining: a brief review," *Engineering*, vol. 3, no. 4, pp. 546–551, 2017.

[4] X.-T. Feng, J. Liu, B. Chen, Y. Xiao, G. Feng, and F. Zhang, "Monitoring, warning, and control of rockburst in deep metal mines," *Engineering*, vol. 3, no. 4, pp. 538–545, 2017.

[5] X. D. Zhao, L. Deng, and J. Xu, "Defining stress thresholds of granite failure process based on acoustic emission activity parameters," *Shock and Vibration*, vol. 2020, Article ID 8812066, 8 pages, 2020.

[6] X. Zhao, H. Li, and S. Zhang, "Analysis of the spalling process of rock mass around a deep underground ramp based on numerical modeling and in-situ observation," *Geomatics, Natural Hazards and Risk*, vol. 11, no. 1, pp. 1619–1637, 2020.

[7] L. Rybach and M. Pfister, "Temperature predictions and predictive temperatures in deep tunnels," *Rock Mechanics and Rock Engineering*, vol. 27, no. 2, pp. 77–88, 1994.

[8] R. P. Suggate, "Relations between depth of burial, vitrinite reflectance and geothermal gradient," *Journal of Petroleum Geology*, vol. 21, no. 1, pp. 5–32, 1998.

[9] Q. Jiang, X.-T. Feng, T.-B. Xiang, and G.-S. Su, "Rockburst characteristics and numerical simulation based on a new energy index: a case study of a tunnel at 2,500 m depth," *Bulletin of Engineering Geology and the Environment*, vol. 69, no. 3, pp. 381–388, 2010.

[10] G. Chen, T. Li, G. Zhang, H. Yin, and H. Zhang, "Temperature effect of rock burst for hard rock in deep-buried tunnel," *Natural Hazards*, vol. 72, no. 2, pp. 915–926, 2014.

[11] S. Li, S. Li, Q. Zhang et al., "Predicting geological hazards during tunnel construction," *Journal of Rock Mechanics and Geotechnical Engineering*, vol. 2, no. 3, pp. 232–242, 2010.

[12] N. F. Liu, N. Li, J. P. Liu, X. C. Yao, and X. G. Guo, "Mechanical characteristics of high-temperature tunnel based on analytical method," *ISRM SINOROCK International Society for Rock Mechanics*, 2013.

[13] Y. S. Zhang, T. Y. Xiong, Y. B. Du et al., "Geostress characteristics and simulation experiment of rockburst of a deep-buried tunnel in Gaoligong mountain," *Chinese Journal of Rock Mechanics and Engineering*, vol. 28, no. 11, pp. 2286–2294, 2009.

[14] J. Yan, C. He, B. Wang, W. Meng, and J. F. Yang, "Prediction of rock bursts for Sangzhuling tunnel located on Lhasa-Nyingchi railway under coupled thermo-mechanical effects," *Journal of Southwest Jiaotong University*, vol. 53, no. 3, pp. 434–441, 2018.

[15] J. Yan, C. He, B. Wang, and W. Meng, "Influence of high geotemperature on rockburst occurrence in tunnel," *Rock and Soil Mechanics*, vol. 40, no. 4, pp. 1543–1550, 2019.

[16] J. Yan, C. He, B. Wang, G. W. Xu, F. Y. Wu, and P. Pan, "Research on characteristics and mechanism of rockburst occurring in high geo-temperature and high geo-stress tunnel," *Journal of the China Railway Society*, vol. 42, no. 12, pp. 186–194, 2020.

[17] X. B. Li and F. Q. Gong, "Research progress and prospect of deep mining rock mechanics based on coupled static-dynamic loading testing," *Journal of China Coal Society*, vol. 46, no. 3, pp. 846–866, 2021.

[18] J. Lu, G. Yin, H. Gao et al., "True triaxial experimental study of disturbed compound dynamic disaster in deep underground coal mine," *Rock Mechanics and Rock Engineering*, vol. 53, no. 5, pp. 2347–2364, 2020.

[19] F. Feng, X. B. Li, L. Luo et al., "Rockburst response in hard rock owing to excavation unloading of twin tunnels at great depth," *Bulletin of Engineering Geology and the Environment*, vol. 80, no. 10, pp. 7613–7631, 2021.

[20] L. Jiang, P. Kong, P. Zhang et al., "Dynamic analysis of the rock burst potential of a longwall panel intersecting with a fault," *Rock Mechanics and Rock Engineering*, vol. 53, no. 4, pp. 1737–1754, 2020.

[21] F. Q. Gong, J. Y. Yan, and X. B. Li, "A new criterion of rock burst proneness based on the linear energy storage law and the residual elastic energy index," *Chinese Journal of Rock Mechanics and Engineering*, vol. 37, no. 9, pp. 1993–2014, 2018.

[22] X. Si, L. Huang, X. Li, C. Ma, and F. Gong, "Experimental investigation of spalling failure of D-shaped tunnel under three-dimensional high-stress conditions in hard rock," *Rock Mechanics and Rock Engineering*, vol. 54, no. 6, pp. 3017–3038, 2021.

[23] H. Wu, D. Ma, A. J. S. Spearing, and G. Y. Zhao, "Fracture response and mechanisms of brittle rock with different numbers of openings under uniaxial loading," *Geomechanics and Engineering*, vol. 25, no. 6, pp. 481–493, 2021.

[24] X. F. Si and F. Q. Gong, "Strength-weakening effect and shear-tension failure mode transformation mechanism of rockburst for finegrained granite under triaxial unloading compression," *International Journal of Rock Mechanics and Mining Sciences*, vol. 131, Article ID 104347, 2020.

[25] K. Peng, H. Lv, F. Z. Yan, Q. L. Zou, X. Song, and Z. P. Liu, "Effects of temperature on mechanical properties of granite under different fracture modes," *Engineering Fracture Mechanics*, vol. 226, Article ID 106838, 2020.

[26] T. B. Li, H. S. Pan, G. Q. Chen, and L. B. Meng, "Physical model tests on thermo-mechanical effects in rockbursts around tunnels," *Chinese Journal of Rock Mechanics and Engineering*, vol. 37, no. 2, pp. 261–273, 2018.

[27] S. Akdag, M. Karakus, A. Taheri, G. Nguyen, and H. Manchao, "Effects of thermal damage on strain burst mechanism for brittle rocks under true-triaxial loading conditions," *Rock Mechanics and Rock Engineering*, vol. 51, no. 6, pp. 1657–1682, 2018.

[28] F. Q. Ren, C. J. Zhu, M. C. He, and C. Zhu, "Temperature effect on granite strain burst based on binocular stereovision technology," *Environmental Earth Sciences*, vol. 78, no. 24, p. 16, 2019.

[29] G. Su, Z. Chen, J. W. Ju, and J. Jiang, "Influence of temperature on the strainburst characteristics of granite under true triaxial loading conditions," *Engineering Geology*, vol. 222, pp. 38–52, 2017.

[30] J. Jiang, G. Su, X. Zhang, and X.-T. Feng, "Effect of initial damage on remotely triggered rockburst in granite: an experimental study," *Bulletin of Engineering Geology and the Environment*, vol. 79, no. 6, pp. 3175–3194, 2020.

[31] Nb/T. 10143–2019, *Technical Code for Rockburst Risk Assessment of Hydropower Projects*, Energy Industry Standard, Beijing, China, 2019.

[32] G. S. Su, Y. J. Shi, X. T. Feng, and J. Q. Jiang, "Acoustic signal characteristics in rockburst process," *Chinese Journal of Rock Mechanics and Engineering*, vol. 6, pp. 1190–1201, 2016.

[33] F. Gong, J. Yan, X. Li, and S. Luo, "A peak-strength strain energy storage index for rock burst proneness of rock materials," *International Journal of Rock Mechanics and Mining Sciences*, vol. 117, pp. 76–89, 2019.

[34] Z. He, F. Gong, and S. Luo, "Evaluation of the rockburst proneness of red sandstone with prefabricated boreholes: an experimental study from the energy storage perspective," *Geomatics, Natural Hazards and Risk*, vol. 12, no. 1, pp. 2117–2154, 2021.

[35] F. Gong, Y. Wang, Z. Wang, J. Pan, and S. Luo, "A new criterion of coal burst proneness based on the residual elastic energy index," *International Journal of Mining Science and Technology*, vol. 31, no. 4, pp. 553–563, 2021.

[36] C. David, B. Menéndez, and M. Darot, "Influence of stress-induced and thermal cracking on physical properties and microstructure of La Peyratte granite," *International Journal of Rock Mechanics and Mining Sciences*, vol. 36, no. 4, pp. 433–448, 1999.

[37] X. Y. Shang, Y. Wang, and R. X. Y. Miao, "Acoustic emission source location from P-wave arrival time corrected data and virtual field optimization method," *Mechanical Systems and Signal Processing*, vol. 163, Article ID 108129, 2022.

[38] R. D. Dwivedi, R. K. Goel, V. V. R. Prasad, and A. Sinha, "Thermo-mechanical properties of Indian and other granites," *International Journal of Rock Mechanics and Mining Sciences*, vol. 45, no. 3, pp. 303–315, 2008.

[39] L. Griffiths, M. J. Heap, P. Baud, and J. Schmittbuhl, "Quantification of microcrack characteristics and implications for stiffness and strength of granite," *International Journal of Rock Mechanics and Mining Sciences*, vol. 100, pp. 138–150, 2017.

[40] J. Y. Zhang, Y. J. Shen, G. S. Yang et al., "Inconsistency of changes in uniaxial compressive strength and p-wave velocity of sandstone after temperature treatments," *Journal of Rock Mechanics and Geotechnical Engineering*, vol. 13, no. 1, pp. 143–153, 2020.

[41] T. Yin, X. Li, K. Xia, and S. Huang, "Effect of thermal treatment on the dynamic fracture toughness of Laurentian granite," *Rock Mechanics and Rock Engineering*, vol. 45, no. 6, pp. 1087–1094, 2012.

[42] S.-Q. Yang, P. Xu, Y.-B. Li, and Y.-H. Huang, "Experimental investigation on triaxial mechanical and permeability behavior of sandstone after exposure to different high temperature treatments," *Geothermics*, vol. 69, pp. 93–109, 2017.

[43] L. N. Y. Wong, Y. Zhang, and Z. Wu, "Rock strengthening or weakening upon heating in the mild temperature range?" *Engineering Geology*, vol. 272, Article ID 105619, 2020.

[44] S. Shao, P. L. P. Wasantha, P. G. Ranjith, and B. K. Chen, "Effect of cooling rate on the mechanical behavior of heated Strathbogie granite with different grain sizes," *International Journal of Rock Mechanics and Mining Sciences*, vol. 70, pp. 381–387, 2014.

[45] S. Liu and J. Xu, "An experimental study on the physico-mechanical properties of two post-high-temperature rocks," *Engineering Geology*, vol. 185, pp. 63–70, 2015.

[46] L. Xu, F. Q. Gong, and Z. X. Liu, "Experimental study on rockburst proneness of pre-heated granite at different temperatures: insights from energy storage, dissipation and surplus," *Journal of Rock Mechanics and Geotechnical Engineering*, vol. 14, no. 5, 2022.

[47] S. Sha, G. Rong, J. Tan, R. H. He, and B. W. Li, "Tensile strength and brittleness of sandstone and granite after high-temperature treatment: a review," *Arabian Journal of Geosciences*, vol. 13, no. 14, pp. 1–13, 2020.

[48] M. N. L. Leroy, F. W. Marius, and N. François, "Experimental and theoretical investigations of hard rocks at high temperature," *Advances in Civil Engineering*, vol. 2021, Article ID 8893944, 21 pages, 2021.

[49] A. Kidybinski, "Bursting liability indices of coal," *International Journal of Rock Mechanics and Mining Science & Geomechanics Abstracts*, vol. 18, no. 4, pp. 295–304, 1981.

[50] G. Q. Chen, T. B. Li, W. Wang, F. Guo, and H. Y. Yin, "Characterization of the brittleness of hard rock at different temperatures using uniaxial compression tests," *Geomech & engineering*, vol. 13, no. 1, pp. 63–77, 2017.

[51] M. C. He, D. Q. Liu, W. L. Gong et al., "Development of a testing system for impact rockburst," *Chinese Journal of Rock Mechanics and Engineering*, vol. 33, no. 9, pp. 1729–1739, 2014.

[52] S. W. Zhou, C. C. Xia, Y. S. Hu, Y. Zhou, and P. Y. Zhang, "Damage modeling of basaltic rock subjected to cyclic temperature and uniaxial stress," *International Journal of Rock Mechanics and Mining Sciences*, vol. 77, pp. 163–173, 2015.

[53] X.-l. Xu, M. Karakus, F. Gao, and Z.-z. Zhang, "Thermal damage constitutive model for rock considering damage threshold and residual strength," *Journal of Central South University*, vol. 25, no. 10, pp. 2523–2536, 2018.

[54] X. L. Xu and M. Karakus, "A coupled thermo-mechanical damage model for granite," *International Journal of Rock Mechanics and Mining Sciences*, vol. 103, pp. 195–204, 2018.

[55] F. Q. Gong, P. L. Zhang, S. Luo, J. C. Li, and D. Huang, "Theoretical damage characterisation and damage evolution process of intact rocks based on linear energy dissipation law under uniaxial compression," *International Journal of Rock Mechanics and Mining Sciences*, vol. 146, Article ID 104858, 2021.

[56] L. Xu, F. Q. Gong, and S. Luo, "Effects of pre-existing single crack angle on mechanical behaviors and energy storage characteristics of red sandstone under uniaxial compression," *Theoretical and Applied Fracture Mechanics*, vol. 113, Article ID 102933, 2021.

[57] M. Z. Gao, J. Xie, Y. N. Gao et al., "Mechanical behavior of coal under different mining rates: a case study from laboratory experiments to field testing," *International Journal of Mining Science and Technology*, vol. 31, no. 5, pp. 825–841, 2021.

[58] X. F. Si and F. Q. Gong, "Rockburst simulation tests and strength-weakening effect of circular tunnels under deep high stresses and internal unloading conditions," *Chinese Journal of Rock Mechanics and Engineering*, vol. 40, no. 2, pp. 276–289, 2021.

[59] L. L Li and F. Q. Gong, "Experimental investigation on the energy storage characteristics of red sandstone in triaxial compression tests with constant confining pressure," *Shock and Vibration*, vol. 2020, Article ID 8839761, 11 pages, 2020.

[60] S. Luo and F. Gong, "Linear energy storage and dissipation laws of rocks under present angle shear conditions," *Rock Mechanics and Rock Engineering*, vol. 53, no. 7, pp. 3303–3323, 2020.

[61] S. Luo and F. Q. Gong, "Linear energy storage and dissipation laws during rock fracture under three-point flexural loading," *Engineering Fracture Mechanics*, vol. 234, Article ID 107102, 2020.

[62] H. P. Xie, M. Z. Gao, R. Zhang et al., "Study on concept and progress of in situ fidelity coring of deep rocks," *Chinese Journal of Rock Mechanics and Engineering*, vol. 39, no. 5, pp. 865–876, 2020.

[63] H. P. Xie, C. B. Li, M. Z. Gao, R. Zhang, F. Gao, and J. B. Zhu, "Conceptualization and preliminary research on deep in situ rock mechanics," *Chinese Journal of Rock Mechanics and Engineering*, vol. 40, no. 2, pp. 217–232, 2021.